

# Spectral line shapes in low frequency turbulent tokamak plasmas

Y. Marandet,<sup>1</sup> H. Capes,<sup>2</sup> L. Godbert-Mouret,<sup>1</sup> M. Koubiti,<sup>1</sup> and R. Stamm<sup>1</sup>

<sup>1</sup>PIIM, Université de Provence, Centre de St-Jérôme F13397 Marseille France

<sup>2</sup>DRFC-CEA, 13018 Saint Paul lez Durance Cedex, France

(Dated: January 31, 2018)

In this paper we investigate the influence of low frequency turbulence on Doppler spectral line shapes in magnetized plasmas. Low frequency refers here to fluctuations whose typical time scale is much larger than those characterizing the atomic processes, such as radiative decay, collisions and charge exchange. This ordering is in particular relevant for drift wave turbulence, ubiquitous in edge plasmas of fusion devices. Turbulent fluctuations are found to affect line shapes through both the spatial and time averages introduced by the measurement process. The profile is expressed in terms of the fluid fields describing the plasma. Assuming the spectrometer acquisition time to be much larger than the turbulent time scale, an ordering generally fulfilled in experiments, allows to develop a statistical formalism. We proceed by investigating the effects of density, fluid velocity and temperature fluctuations alone on the Doppler profile of a spectral line emitted by a charge exchange population of neutrals. Line wings are found to be affected by ion temperature or fluid velocity fluctuations, and can in some cases exhibit a power-law behavior. This study gives some insights in the appearance of non-Boltzmann statistics, such as Lévy statistics, when dealing with averaged experimental data.

PACS numbers: 32.70.Jz, 52.35.Ra, 05.40.Fb, 05.40.-a

## I. INTRODUCTION

Spectral line shape studies have played a major role in the investigation of the nature of atomic radiators and their environment, in astrophysics as well as in laboratory plasmas. Indeed, depending on the dominant line broadening mechanisms, it is for instance possible to retrieve the electron density or the ion temperature from the analysis of a given line. However, in many cases actual plasmas are far from thermal equilibrium, being inhomogeneous or having non-Maxwellian velocity distributions, features which significantly complicate the analysis of experimental data. In addition, these departures from thermal equilibrium can trigger instabilities, whose growth and non-linear saturation eventually lead to the onset of turbulence [1, 2, 3]. The importance of investigating the possible effects that turbulence might have on line shapes has been acknowledged very early, and the motivations of these studies were, and still are, two-fold : first there is the need to quantify the errors introduced by neglecting turbulence in routine diagnosis based on line-shapes. Then, the possible existence of significant deviations could be used to diagnose turbulence itself. An optical diagnostic of turbulence based on passive spectroscopy would indeed be very convenient, this sustainable technique being already available on numerous experiments.

Historically, a large number of papers ([4, 5] and references therein) have dealt with the Stark effect resulting from turbulent electric fields, such as those associated to a high supra-thermal level of Langmuir waves [6]. Starting from the seminal paper by Mozer and Baranger [7], several models have been devised to include turbulent Stark broadening in the calculation of line-shapes. The results thus obtained are relevant to plasmas for

which Stark effect is dominant compared to Doppler effect. There are however situations for which this ordering is reversed, and important examples are edge plasmas of magnetic fusion devices such as Tokamaks in the ionizing regime. For these low density plasmas ( $N_e \leq 5 \times 10^{20} \text{ m}^{-3}$ ), Zeeman and Doppler effects are the dominant broadening mechanisms for low lying lines such as the  $D\alpha$  (transition between the levels  $n = 3$  and  $n = 2$  of the atomic deuterium). In such cases, line shape studies essentially provide measurement of the emitters velocity distribution, and have so far brought valuable results concerning the origin of neutrals in edge plasmas [8, 9, 10, 11]. However, these plasmas are known to be strongly turbulent, i.e. the level of fluctuation of the fluid fields characterizing the plasma can rise up to several tenths of percents [2]. The experimental characterization of these fluctuations is of first importance to analyse drift-wave (DW) turbulence, which is held responsible for the so called anomalous transport degrading the quality of the confinement [3].

As an example, we will consider the case of the Balmer  $\alpha$  of hydrogen isotopes ( $D\alpha$  for the case of deuterium), since it is one of the most routinely monitored line in edge plasmas, being both intense and optically thin. In sections II and III, the expression of the measured line profile is carefully discussed to emphasize the role of the spatial and time averages involved in the measure. We show in section II that a neutral population created by charge exchange can be considered as being in a local equilibrium characterized by the local density, temperature and fluid velocity of the ions. In sections IV and V, we will show that in presence of low frequency turbulence, the Doppler profile gives access to an apparent velocity distribution. By further developing the model only briefly presented in [12, 13], this apparent VDF is reex-

pressed in terms of the Probability Distribution Function (PDF) of the fluid fields. In section VI, the influence of density, fluid velocity and temperature are successively investigated in details. Finally, it is shown in section VII that for particular choices of the statistical properties of the turbulent fluctuations, the apparent VDF becomes a Lévy distribution. This result establishes a clear connection with one of our previous work [14], in which we investigated the possible origin of a power law behavior observed in the line wings of  $D\alpha$  spectra measured in the former ergodic divertor configuration of the Tore Supra Tokamak.

## II. EXPRESSION OF THE MEASURED SPECTRA

Let us first define precisely the observable quantity for a spectrally resolved passive spectroscopy measurement. First of all, obtaining the spectrum emitted by the plasma (which will be referred to as the measured spectrum in the following) from the raw spectrum involves deconvolution of the apparatus function  $\mathcal{I}_{ap}$ . In practice, the theoretical spectrum is convolved with  $\mathcal{I}_{ap}$  before being compared to the raw spectrum. The radiation emitted by the plasma is integrated both along the Line Of Sight (LOS) and during the acquisition time of the spectrometer, denoted by  $\tau_m$ . The observable intensity  $\mathcal{I}_{mes}(\Delta\lambda)$ , where  $\Delta\lambda$  stands for the wavelength detuning from the center of the line, is thus given by the following expression

$$\mathcal{I}_{mes}(\Delta\lambda) = \int_0^{\tau_m} \int_{\mathcal{L}} \mathcal{I}_{loc}(\Delta\lambda, z, t) \frac{\delta S}{4\pi z^2} dz dt, \quad (1)$$

where  $\mathcal{I}_{loc}(\Delta\lambda, z, t)$  is the local line shape emitted at a given distance  $z$  from the detector along the LOS  $\mathcal{L}$ . Here  $\delta S$  stands for the detector active area. Assuming the latter to be delimited by  $z_1 < z_2$  such that  $L = z_2 - z_1 \ll z_1$ , Eq. (1) reduces to

$$\mathcal{I}_{mes}(\Delta\lambda) \simeq \frac{\delta S}{4\pi z_1^2} \int_0^{\tau_m} \int_{z_1}^{z_2} \mathcal{I}_{loc}(\Delta\lambda, z, t) dz dt. \quad (2)$$

We now introduce the local absolute brightness

$$b(z, t) = \int_{-\infty}^{+\infty} \mathcal{I}_{loc}(\Delta\lambda, z, t) d\Delta\lambda, \quad (3)$$

and define the local line shape normalized to unity by  $\mathcal{I}(\Delta\lambda, z, t) = \mathcal{I}_{loc}(\Delta\lambda, z, t)/b(z, t)$ . In the remainder of this paper, we will deal with the measured profile normalized to unity, given by

$$\mathcal{I}_{mes}(\Delta\lambda) = \frac{1}{\tau_m} \int_0^{\tau_m} \frac{1}{L} \int_{z_1}^{z_2} B(z, t) \mathcal{I}(\Delta\lambda, z, t) dz dt. \quad (4)$$

where the relative brightness  $B$  is defined by

$$B(z, t) = \frac{b(z, t)}{\frac{1}{\tau_m} \int_0^{\tau_m} \frac{1}{L} \int_{z_1}^{z_2} b(z, t) dt dz} \quad (5)$$

So, the measurement process both entails a spatial and a time average of the local profile. In order to achieve time resolved measurements, the acquisition time  $\tau_m$  should be chosen shorter than the typical turbulent time, which is associated to the time variations of the functions  $B(z, t)$  and  $\mathcal{I}(\Delta\lambda, z, t)$ . However, such a choice would generally result in spectra having very low signal to noise ratios. To retrieve information from time resolved measurements, one must then either forsake spectral resolution or resort to active techniques, such as Beam Emission Spectroscopy (BES), which allows to diagnose the time behavior of turbulent density fluctuations at the edge of tokamaks (e.g. [15, 16]). Conversely, if spectral resolution is needed, the acquisition time should be sufficiently large so as to ensure reasonable signal to noise ratios. In this paper we will deal with the latter situation, for the limiting case in which the acquisition time is much larger than the typical turbulent time scale. In fact, this generally corresponds to the actual situation for passive spectral line shapes measurements. Spectra thus obtained will prove to yield further information than time resolved experiments. The next step in the modelling consists in relating the local brightness  $B$  and the local profile  $\mathcal{I}$  to the parameters characterizing the plasma.

## III. MODELLING OF THE LOCAL PROFILE

In this section we will first describe the model that will be used to describe the plasma, i.e. a set of fluid equations. The remainder of the section will present the expressions of the local brightness and profile relevant to edge plasmas typical conditions.

### A. Plasma description

We are interested in plasmas which can be described by a set of  $N$  macroscopic fields denoted by  $\mathbf{X} = \{X_1(\mathbf{r}, t), \dots, X_N(\mathbf{r}, t)\}$ , including the density, temperature and fluid velocity for each species. These fields are solutions of a set of fluid equations. For example, the field  $X_i(\mathbf{r}, t)$  would satisfy to a conservation equation

$$\frac{\partial X_i}{\partial t} + \nabla \cdot \mathbf{\Gamma} = S(\mathbf{X}), \quad (6)$$

where  $S(\mathbf{X})$  is a source term and  $\mathbf{\Gamma}$  is a flux, for example given by the sum of a diffusive and a convective flux  $\mathbf{\Gamma} = -\kappa \nabla X_i + \mathbf{u} X_i$ ,  $\mathbf{u} = X_j$  being a velocity field. It is furthermore assumed that this set of fluid equations describes a turbulent stationary state, for which the statistical properties of the plasma do not change during the

acquisition time  $\tau_m$ . For each species, the validity of a fluid description relies on the ordering  $\tau \gg \nu_{coll}^{-1}$ , where  $\tau$  is the typical time of variation of the fluid fields and  $\nu_{coll}$  the collision frequency (in the case of DW turbulence in edge plasmas, we have  $\tau \simeq 10 - 100 \mu s$ ). The fulfillment of this ordering ensures that the VDF  $F_\gamma$  of the species  $\gamma = i, e$  remains close to a local Maxwellian at each time and location

$$F_\gamma(\mathbf{v}, \mathbf{r}, t) \simeq \sqrt{\frac{m_\gamma}{2\pi T_\gamma(\mathbf{r}, t)}} \exp\left(-\frac{m_\gamma(\mathbf{v} - \mathbf{u}_\gamma(\mathbf{r}, t))^2}{2T_\gamma(\mathbf{r}, t)}\right), \quad (7)$$

where  $m_\gamma$ ,  $T_\gamma(\mathbf{r}, t)$  and  $\mathbf{u}_\gamma(\mathbf{r}, t)$  are respectively the mass, the temperature field expressed in eV, and the fluid velocity field of the species labeled by  $\gamma$ . In the following, we shall consider the case of a pure deuterium plasma for which  $Z_{eff} = 1$ .

The calculation of the neutrals VDF requires the use of a refined model. Indeed, there are different sources of neutrals in edge plasmas of tokamaks, each of them giving birth to a single class of neutrals. These classes, characterized by different temperatures, coexist since the density is usually too low in order to ensure their complete relaxation toward the background local equilibrium. The lowest temperature class originates from the dissociation of molecules released from the wall, whereas those having larger temperatures are mainly attributed to charge exchange reactions (e.g. [8, 9, 10, 11]). In the following, we will only consider the class of neutrals locally created by charge exchange reactions, that plays an important role for the line wings behavior. Indeed, it will be shown that turbulence essentially affects these regions of the spectra. In order to model the VDF of these emitters, we can once again take advantage of the separation of scales between atomic processes and turbulence. In fact, the inverse of the charge exchange rate is of the order of a few  $\mu s$ , i.e. shorter than the typical turbulent time scale. As a result, the emitters VDF remains at each time close to that of the ions, given by Eq. (7) with  $\gamma = i$ . From the microscopic point of view, the emitter's VDF thus appears as a Maxwellian characterized by a set of slowly varying macroscopic fields.

### B. The local brightness

The local line brightness is directly related to the population of the transition upper atomic level. In general, this population has to be calculated by taking into account the contributions of the different processes (for instance collisions, charge exchange, radiative decay) populating or depopulating the levels. If the fluid fields characterizing the plasma vary slowly on the typical time scales associated to these processes, a stationary approach is suitable to calculate the brightness. The levels populations are assumed to be time independent and are calculated using the values of the

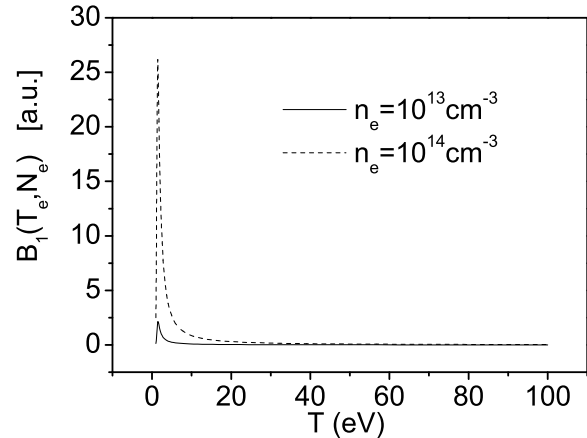


FIG. 1: plot of the brightness per emitter as a function of the electronic temperature  $T_e$  in the range 0 to 100 eV for a given density  $N_e = 10^{18} \text{ m}^{-3}$ . The temperature dependence is weak for  $T_e > 15$  eV.

fields  $\mathbf{X}(\mathbf{r}, t)$  at each time and location. In practice, the brightness essentially depends on the electron density  $N_e(\mathbf{r}, t)$  and temperature  $T_e(\mathbf{r}, t)$ . We have performed a calculation of the brightness per emitter  $B_1$  (defined as  $B(\mathbf{r}, t) = n_0(\mathbf{r}, t)B_1(\mathbf{X}(\mathbf{r}, t))$ , where  $n_0(\mathbf{r}, t)$  is the density of emitters) for the  $D_\alpha$  line in edge plasma conditions, i.e.  $N_e = 10^{18} - 10^{19} \text{ m}^{-3}$  and  $T_e = 1 - 100$  eV, using the code SOPHIA [17]. The electron density dependence of  $B_1$  is found to be linear, in accordance with the fact that the upper level of the transition is essentially populated by electronic collisions from the ground state. This leads to a quadratic behavior of the brightness with  $N_e$ , since  $n_0 \propto N_e$ . The influence of the electron temperature on the brightness is more subtle, as shown on Fig. 1 for two different densities. The existence of a maximum reflects the competition between the growth of the electron collisions cross section with temperature, which dominates the small temperatures behavior, and the ionisation process. For electron temperatures larger than 15 eV, the influence of  $T_e$  on the brightness is weak, and in the remainder of this paper, we shall therefore consider the brightness as being only a function of the electron density.

### C. The local line shape

The  $\Delta\lambda$  dependance of the local profile  $\mathcal{I}(\Delta\lambda, z, t)$  is determined by the dominant line broadening mechanisms. In magnetized plasmas, Zeeman, Stark and Doppler broadenings should *a priori* be taken simultaneously into account. In general, the local profile normalized to unity can be written as the following convolution

product

$$\mathcal{I}(\Delta\lambda, z, t) = \int d\Delta\lambda' I_{ZS}(\Delta\lambda - \Delta\lambda', z, t) I_D(\Delta\lambda, z, t), \quad (8)$$

where  $I_{ZS}$  is the local Zeeman-Stark profile, which describe the broadening resulting from the effect of the magnetic and electric fields on the emitters energy levels [4]. The Doppler profile  $I_D$  is related to the wavelength shift introduced by the movement of the radiator along the LOS, and is thus directly given by

$$I_D(\Delta\lambda, z, t) d\Delta\lambda = f(v_z, z, t) dv_z, \quad (9)$$

where  $f(v_z, z, t)$  stands for the emitters VDF along the LOS, obtained from (7) upon integrating over the two components of the velocity perpendicular to the LOS

$$f(v_z, z, t) = \int \int dv_x dv_y F(\mathbf{v}, z, t). \quad (10)$$

It should be noted that Eq. (9) would not be valid if the velocity of the emitter were not constant during the emission process, due to collisions [18]. If  $\Delta\omega_D$  denotes the Doppler line width expressed in units of pulsation, Eq. (9) assumes that  $\tau_{coll}^{-1} \ll \Delta\omega_D$ . This ordering is largely satisfied in edge plasmas, and is moreover not inconsistent with the assumption  $\tau_{col} > \tau$  underlying the validity of Eq. (7). For a given line, the relative importance of the different broadening mechanisms depends on plasma conditions, i.e. on the average values taken by the plasma density and temperature, but also on the detuning  $\Delta\lambda$ . In the following, we will again discuss the case of the  $D\alpha$  line, first for the bulk of the line and

then for line wings, these regions of the spectra for which  $|\Delta\lambda| \gg \Delta\lambda_{1/2}$ ,  $\Delta\lambda_{1/2}$  being the HWHM of the profile. In the center of the line, Stark effect is negligible for densities lower than  $N_e = 5 \times 10^{20} \text{ m}^{-3}$ , an ordering which is usually (but not always) satisfied in edge plasmas. In addition, since the magnetic field is larger than 1 T, fine structure can be neglected [19]. Therefore, the  $D\alpha$  line splits into three Doppler-broadened Zeeman components (one  $\pi$  and two  $\sigma$ ). The lateral  $\sigma$  components are equally separated from the central  $\pi$  component. Under parallel observation with respect to the magnetic field, only the  $\sigma$  components are observable. Although negligible in the bulk of the line, Stark effect might become dominant in the line wings for detunings larger than a value  $\Delta\lambda_S(N_e)$  which is an increasing function of the density. Therefore, in the remainder of the paper it should be understood that the Doppler line wings are the regions of the spectra for which both orderings  $|\Delta\lambda| \gg \Delta\lambda_{1/2}$  and  $|\Delta\lambda| < \Delta\lambda_S$  are simultaneously valid. The existence of such a regime depends on the plasma conditions. Its study is relevant for edge plasmas and consequently Stark effect will be neglected in the remainder of the paper. However, it should be emphasized that the statistical formalism which is developed in section V would also be applicable if Stark effect were not negligible. In the latter case, the local profile should be calculated using Eq. (8) instead of Eq. (9).

According to Eq. (9), the Doppler spectrum of a single Zeeman component is proportional to the emitters VDF  $f$  along the line of sight. As previously explained, we consider a class of neutrals created by charge exchange reactions, whose VDF is approximated by a local Maxwellian. The corresponding expression of the local Doppler profile is given by

$$\mathcal{I}_D(\Delta\lambda, T(\mathbf{r}, t), u_z(\mathbf{r}, t)) = \sqrt{\frac{m}{2\pi T(\mathbf{r}, t)}} \exp\left(-\frac{m(\Delta\lambda - \frac{\lambda_0}{c} u_z(\mathbf{r}, t))^2}{\frac{2\lambda_0}{c} T(\mathbf{r}, t)}\right), \quad (11)$$

where  $m$  is the emitters mass,  $\lambda_0$  the unperturbed wavelength of the transition under study,  $T(\mathbf{r}, t)$  the ion temperature, and  $u_z(\mathbf{r}, t)$  the component of the ion fluid velocity along the LOS.

#### IV. APPARENT VELOCITY DISTRIBUTION

Gathering the results of the above sections, we obtain the following expression for the measured profile normal-

ized to unity

$$\mathcal{I}_{mes}(\Delta\lambda) = \frac{1}{\tau_m} \int_0^{\tau_m} dt \frac{1}{L} \int_{\mathcal{L}} dz B(\mathbf{X}(z, t)) I_D(\Delta\lambda, \mathbf{X}(z, t)), \quad (12)$$

which is now expressed in terms of the fluids fields describing the plasma. The *apparent velocity distribution function*  $f_a(v_z)$  is straightforwardly deduced from the measured spectrum by

$$\mathcal{I}_{mes}(\Delta\lambda) d\Delta\lambda = f_a(v_z) dv_z, \quad (13)$$

in analogy with Eq.(9). This VDF is an average of the

local emitters VDF over time and space. Indeed, combining Eq. (12) and Eq. (13) leads to the following explicit expression

$$f_a(v_z) = \frac{1}{\tau_m} \int_0^{\tau_m} dt \frac{1}{L} \int_{\mathcal{L}} dz B(\mathbf{X}(z, t)) f(v_z, \mathbf{X}(z, t)). \quad (14)$$

The apparent VDF  $f_a$  can be given a deep physical meaning as will be shown in section VII.

Intuitively, in plasmas where the fluctuation rate is low,  $f_a$  should remain close to a Maxwellian  $f_{eq}$  characterized by the time and space averaged values of the temperature and the velocity fields, respectively denoted by  $\bar{T}$  and  $\bar{u}_z$ , i.e

$$f_a(v_z) \simeq f_{eq}(v_z; \bar{T}, \bar{u}_z). \quad (15)$$

Conversely, in a situation where strong fluctuations occur, there is *a priori* no obvious reason for which the apparent velocity distribution should remain close to the average Maxwellian given by Eq. (15). In particular, in edge plasmas the fluctuation rate can rise up to several tenths of percents. The validity of Eq. (15) then clearly becomes questionable, and Eq. (14) should be used instead. A calculation of the apparent VDF  $f_a$  can be carried out from the latter equation once the solutions of the fluid equations are known, i.e. the time and space dependences of each of the fields  $X_i(\mathbf{r}, t)$  have been worked out. Due to the non-linear nature of the fluid

equations and the complexity of the geometry, this calculation would best be achieved numerically. Although such an approach might be able to encompass the complexity of the problem, we find it worthwhile to begin with a simpler one in order to gain insights on the kind of effects that turbulence might produce on spectral line shapes.

## V. STATISTICAL FORMALISM

### A. Expression of the profile

In the following, we will take advantage of the fact that the acquisition time of the spectrometer is usually much larger than the typical time scale of the turbulence  $\tau$ . Let us first note that upon using an appropriate normalisation for the  $\delta$  function, the following relation holds for any  $z$  and  $t$

$$\int_N \prod_{i=1}^N \delta(\bar{X}_i - X_i(z, t)) d\bar{X}_1 \dots d\bar{X}_N = 1, \quad (16)$$

where  $\bar{X}_i$  is the sample space variable corresponding to the field  $X_i(z, t)$ . Introducing this identity into Eq. (14), interchanging the order of time and sample space integrations, and finally making use of the delta function sifting property yields the following expression for the apparent velocity distribution function

$$f_a(v_z) = \frac{1}{L} \int_{\mathcal{L}} dz \int_N d\bar{X}_1 \dots d\bar{X}_N \left[ \frac{1}{\tau_m} \int_0^{\tau_m} \prod_{i=1}^N \delta(\bar{X}_i - X_i(z, t)) dt \right] B(\bar{\mathbf{X}}) f(v_z, \bar{\mathbf{X}}). \quad (17)$$

The quantity between brackets is a time average of the delta functions product, whose typical time variations occur on the time scale  $\tau \ll \tau_m$ . It is therefore justified to let  $\tau_m$  tend to infinity [20], and then use the ergodic assumption, i.e. replace the time average by an ensemble average denoted by the brackets  $\langle \cdot \rangle$

$$\lim_{\tau_m \rightarrow +\infty} \frac{1}{\tau_m} \int_0^{\tau_m} \prod_{i=1}^N \delta(\bar{X}_i - X_i(z, t)) dt = \left\langle \prod_{i=1}^N \delta(\bar{X}_i - X_i(z, t)) \right\rangle. \quad (18)$$

This ensemble average has to be understood as an average over the time realisations of the stochastic fields  $X_i(t, z)$  at point  $z$ , assumed to be a stationary process. Introducing the local joint Probability Density Function (PDF) of the fluctuating fields defined by

$$\mathcal{P}(\bar{X}_1, \dots, \bar{X}_N, z) = \left\langle \prod_{i=1}^N \delta(\bar{X}_i - X_i(z, t)) \right\rangle, \quad (19)$$

the apparent VDF becomes

$$f_a(v_z) = \frac{1}{L} \int_{\mathcal{L}} dz \int_N d\bar{\mathbf{X}} \mathcal{P}(\bar{\mathbf{X}}, z) B(\bar{\mathbf{X}}) f(v_z, \bar{\mathbf{X}}). \quad (20)$$

Finally, upon integrating on the space coordinate  $z$ , the

apparent VDF is given by

$$f_a(v_z) = \int_N d\bar{\mathbf{X}} W(\bar{\mathbf{X}}) B(\bar{\mathbf{X}}) f(v_z, \bar{\mathbf{X}}), \quad (21)$$

where the spatially integrated PDF  $W(\bar{\mathbf{X}})$  is obtained from

$$W(\bar{\mathbf{X}}) = \frac{1}{L} \int_{\mathcal{C}} dz \mathcal{P}(\bar{\mathbf{X}}, z). \quad (22)$$

In the remainder of the paper we shall furthermore assume homogeneous turbulence, that is  $W(\bar{\mathbf{X}}) \equiv \mathcal{P}(\bar{\mathbf{X}}, z)$  (note that the weaker assumption of homogeneity along the line of sight is sufficient).

## B. Discussion

In the frame of our statistical reformulation, it is no longer necessary to know the solutions of the fluid equations in order to calculate the apparent VDF. Instead, the joint PDF of the turbulent fields should have been computed. A straightforward approach would be to rely on a fluid code, so as to compute histories of the different fields, and then their PDF. As we have already pointed out, this would require heavy numerical computation, especially in order to obtain the PDF tails with a good accuracy. Furthermore, if such calculations were carried out, any statistical reformulation would obviously be superfluous, and the apparent VDF could directly be obtained from Eq. (14). An approach more suited to our formalism should proceed directly at the PDF level. The next section will be devoted to present such a model, initially developed by Pope [21]. However, it should be emphasized that such a calculation is bypassed if assumptions for the shape of the PDF are made. This is the one of the advantages of our formalism, since it allows to draw conclusions on the properties that turbulence should have so as to significantly affect line shapes.

## C. Determination of the PDF from the fluid equations

Let us consider the passive advection of a scalar  $X(z, t)$  solution of Eq. (6), in which the source term is an arbitrary function of  $X$  and the flux  $\mathbf{\Gamma}$  is the sum of a convective term and a diffusive term. The convective velocity field  $\mathbf{u}$  is assumed to be an incompressible stochastic field, the statistical properties of which are known. In order to calculate the apparent velocity distribution function from Eq. (21), the spatially integrated joint PDF of velocity and temperature, denoted by  $W(\mathbf{u}, \bar{X})$ , should be calculated. Here, we will limit ourselves to the modelling of the marginal distribution  $W(\bar{X})$ , obtained by integrating  $W(\mathbf{u}, \bar{X})$  over the velocity. Indeed, this will

be sufficient to highlight the salient points of the model. Assuming homogeneous turbulence, and then following Pope [21], the time dependent PDF  $W(\bar{X}, t)$  is shown to obey a Fokker-Planck like equation

$$\frac{\partial W}{\partial t} = \frac{\partial}{\partial \bar{X}} [S(\bar{X})W] - \frac{\partial^2}{\partial \bar{X}^2} [D(\bar{X})W], \quad (23)$$

where  $S(\bar{X})$  is the source term in the fluid equation. The expression of the function  $D(\bar{X})$  will be discussed below. The stationary solution of the latter equation is

$$W(\bar{X}) = \frac{C}{D(\bar{X})} \exp\left(-\int_0^{\bar{X}} \frac{S(w)}{D(w)} dw\right). \quad (24)$$

As a result, in the PDF approach a non-linear source term  $S$  does not introduce any closure problem, unlike in the moment based models [1]. The problem remains nonetheless unclosed, since the function  $D(\bar{X})$  is in general not expressible in terms of  $W(\bar{X})$  or  $S(\bar{X})$  alone. Indeed, the shape of this function depends on the correlations between  $X$  and its gradient. More precisely, it can be recast in the following form

$$D(\bar{X}) = \frac{1}{\langle \nabla \bar{X} \rangle^2} \int d(\nabla \bar{X}) \mathcal{P}(\nabla \bar{X} | \bar{X}) (\nabla \bar{X})^2, \quad (25)$$

where  $\mathcal{P}(\nabla \bar{X} | \bar{X})$  is the PDF of the gradient of  $X$ , conditioned to a given value of  $X$  [21]. In order to obtain this PDF, an equation for the joint PDF of  $X$  and its gradient should be written [22], which in turn would involve correlations with higher orders gradients. Eventually, one ends up with an infinite hierarchy of equations, involving the joint PDFs of  $X, \nabla X, \nabla^2 X, \dots$ . In addition, it should be kept in mind that the statistical properties of the velocity field  $\mathbf{u}$ , while not appearing explicitly in Eq. (24), do actually affect the shape of  $D(\bar{X})$  through Eq. (6), as should the expression of  $S(X)$ . The closure of this hierarchy has proven to be difficult to address. Promising techniques, such as the *mapping closure* [22] have not yet led to decisive results (for an application to the Hasegawa-Mima equation governing plasma turbulence, see Ref. [23]). Addressing these issues is largely beyond the scope of the present paper, and for our purposes it will be sufficient to present an early attempt to this closure problem, due to Sinai and Yakhot [24]. These authors were interested in the case of passive advection of temperature in homogeneous decaying turbulence, for which there is no source term in the temperature equation. Their idea is to deal with the rescaled quantity  $X = T/\langle T^2 \rangle$ , which is solution of an equation analogous to (6),  $S(\bar{X})$  being a linear function of  $\bar{X}$ . The following Taylor development is used to express the function  $D(\bar{X})$

$$D(\bar{X}) \simeq 1 + k\bar{X}^2, \quad (26)$$

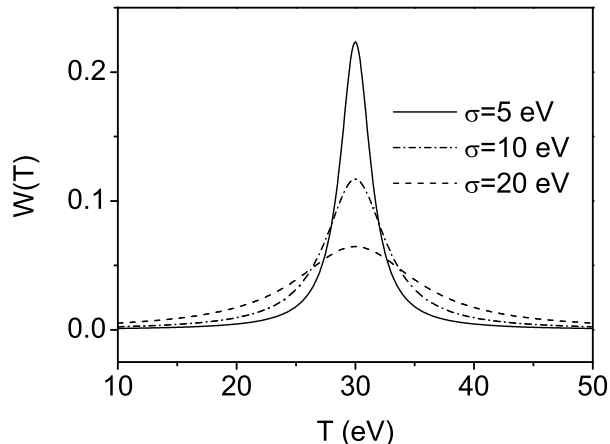


FIG. 2: Plot of the Sinai PDF for  $T_0 = 30$  eV,  $k = 10$  and for different values of  $\sigma = 5, 10, 20$  eV. These distributions are used to compute the corresponding apparent VDF on Fig. 6

where the parameter  $k > 0$  is a measure of the correlations strength. From Eq. (24), the following result for the temperature PDF is readily obtained

$$W(T) = \frac{C}{\left(1 + k \left(\frac{T-T_0}{\sigma}\right)^2\right)^{1+1/2k}}, \quad (27)$$

where  $C$  is a normalization constant, and  $\sigma$  controls the width of the distribution. Fig. 2 shows a plot of  $W(T)$  for  $T_0 = 30$  eV,  $k = 10$  and  $\sigma = 5, 10, 20$  eV. A few subtleties and limitations concerning the use of this result deserve to be mentioned. First, it should be noted that  $\sigma$  is actually time dependant. We shall assume here that the acquisition time  $\tau_m$  is chosen such that  $\sigma/\dot{\sigma} \ll \tau_m$ . This requires a separation of time scales between the turbulent fluctuations and the decay of the average quantities. Secondly, the correlations are treated using the development given by Eq. (26), which is not valid for large values of the temperatures. Our results concerning line wings should thus be limited to not too large detuning  $\Delta\lambda$ . Finally, it should be pointed out that the distribution given by Eq. (27) is a Tsallis distribution (e.g. [25]) with  $q = (1 + 2k)^{-1}$ . Therefore, in this model, temperature fluctuations obey to Tsallis non-extensive statistical mechanics [25] when correlations exist, and to Boltzmann statistics for vanishing correlations.

In the next section, we shall use these results as an input for apparent VDF calculations.

## VI. APPLICATION TO THE CASE OF ONE FLUCTUATING VARIABLE

In an actual turbulent plasma, several fields fluctuate, and these fluctuations are coupled. According to Eq. (21), the joint PDF of the relevant fields should be computed before calculating the apparent VDF. However, the role of density, velocity and temperature fluctuations on the apparent VDF shape have no reason to be identical. As a first approximation, it is therefore rational to consider the idealized case in which only one field fluctuates. This will shed light on which field fluctuations lead to the most significant effects on line shapes.

### A. Density fluctuations

Let us first consider density fluctuations. Since the local VDF normalized to unity does not depend on density, the integration over density fluctuations is trivially performed, and the apparent VDF is found to be equal to the local emitters VDF

$$f_a(v_z) = \int_0^{+\infty} dn B(n) W(n) f(v_z, T) = f(v_z, T). \quad (28)$$

Therefore, at this level of approximation, Doppler line shapes are not sensitive to density fluctuations. The apparent VDF should thus remain Gaussian with the temperature  $T$ , whatever the shape of  $W(n)$ . This is in sharp contrast with line brightness time resolved measurements, which essentially provide information on density fluctuations. However, it should be noted that for cases in which Stark effect is not negligible, Eq. (28) no longer holds, since the local line shape then strongly depends on the density. As we have already pointed out, the formalism presented here could nevertheless be used upon replacing the local Doppler profile by the total profile given by Eq. (8).

### B. Fluid velocity fluctuations

Let us now investigate the case in which only the fluid velocity fluctuates. In the following,  $W(u_z)$  stands for the PDF of the fluid velocity component along the line of sight, and  $\sigma_u^2$  for its variance. Starting from Eq. (21), the apparent VDF reduces to

$$f_a(v_z) = \int W(u_z) f(v_z - u_z, T) du_z, \quad (29)$$

which is the convolution product of  $W$  and the local Maxwellian. Eq. (29) is a well known result in plasma spectroscopy, which is mentioned in classical textbooks [26]. A shape-independent definition of the apparent

temperature  $T_{eff}$  from the profile should proceed from its second moment

$$\xi T_a = \int_{-\infty}^{+\infty} f_a(v_z) v_z^2 dv. \quad (30)$$

In the fluctuations-free case, the actual temperature of the emitters  $T$  is recovered, whereas if fluctuations do occur the apparent temperature is given by

$$T_a = T \left[ 1 + \frac{\sigma_{u_z}^2}{v_{th}^2} \right], \quad (31)$$

where  $v_{th}$  is the thermal velocity corresponding to the temperature  $T$ . The apparent temperature obtained from the Doppler line width is thus not rigorously equal to the actual temperature of the emitters. This result has already been mentioned by several authors, and was actually used in the first models retaining the effect of turbulence on Doppler line shapes [27]. In order to obtain a ten percents discrepancy between  $T_a$  and  $T$  for deuterium emitters, the fluctuation rate should be of the order of thirty percents (i.e.  $\sigma_u \sim 0.3 v_{th}$ ). This effect would be stronger for heavy emitters, since their thermal velocity is smaller [26]. This estimation suggests that the  $D_\alpha$  line width is not strongly modified by fluid velocity fluctuations. However, considering only the line width is not sufficient. In fact, the line shape, i.e. the apparent VDF, is often found to be non-Gaussian, and therefore from Eq. (29), so should be the PDF  $W(u_z)$ . Recent findings in astrophysical spectra [28, 29, 30], as well as in tokamak plasmas for radial velocity fluctuations [31] indicate strong deviations from the Maxwellian, especially for line wings. As an illustration, let us consider PDFs which have power law tails characterized by an exponent  $\alpha$  such that  $0 < \alpha < 2$ . It is easily shown from Eq. (29) that the resulting apparent VDF features a similar asymptotical dependence

$$f_a(v_z) \propto \frac{1}{|v_z|^{\alpha+1}}. \quad (32)$$

Such a behavior would for instance arise if the velocity PDF were a Lévy distribution (see section V). Examples of these distributions are plotted on Fig. 3, for  $\alpha = 0.5, 1, 1.5$  and  $c^\alpha = v_{th}/10$ . The resulting apparent velocity are plotted on Fig. 4, and exhibit a power-law behavior in their tails. However, it should be pointed out that for this effect to be observable, large amplitude velocity fluctuations of the order of a few thermal velocity  $v_{th}$  should actually occur. Finally, it should be noted that in a magnetized plasma, the physics underlying parallel and perpendicular velocity fluctuations are different. The latter are related to the electric field fluctuations through

$$\mathbf{u}_\perp \simeq \frac{\mathbf{E} \times \mathbf{B}}{B^2}, \quad (33)$$

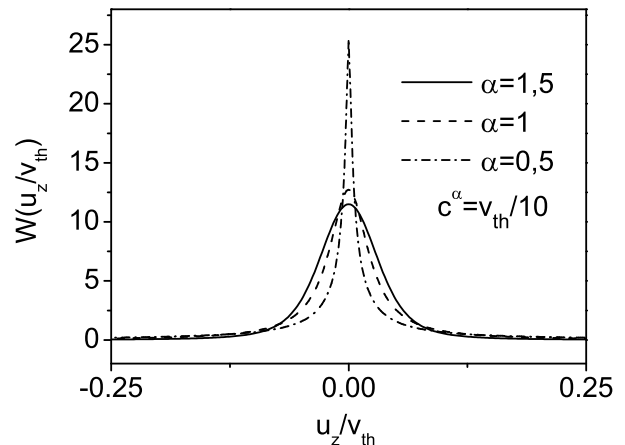


FIG. 3: Plot of the Lévy velocity PDF for  $\alpha = 0.5, 1, 1.5$ . The fluid velocity is plotted in units of the thermal velocity  $v_{th}$ . The parameter  $c$  characterizing the width of the distribution (see section V) is defined by  $c^\alpha = v_{th}/10$ .

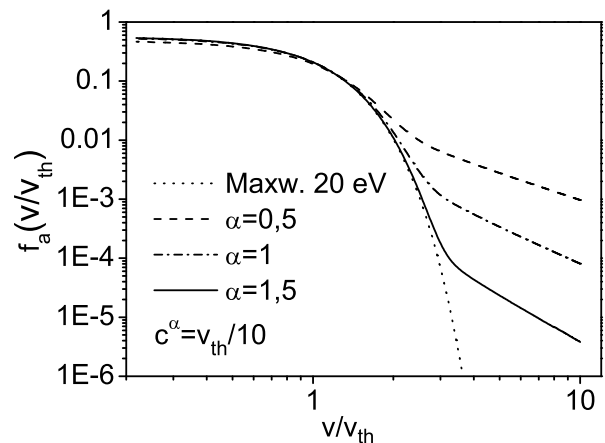


FIG. 4: Plot of the apparent velocity distribution corresponding to Lévy velocity PDF in a logarithmic scale. The dotted line corresponds to the Maxwellian which would be observed in the absence of fluctuations. The velocity is plotted in units of the thermal velocity  $v_{th}$ . The existence of an algebraic decay of exponent  $-\alpha + 1$  in the tail of the apparent VDF is clearly seen.

whereas the former can arise from a Kelvin-Helmholtz like instability associated to the existence of a perpendicular gradient of parallel velocity. Changing the orientation of the line of sight would allow to investigate each of these different cases.

### C. Temperature fluctuations

Finally, we consider the case where only the ion temperature fluctuates, and for which the apparent VDF

reads

$$f_a(v_z) = \int_0^{+\infty} W(T) f(v_z, T) dT. \quad (34)$$

The latter is not a convolution product, in opposition to the case of velocity fluctuations. To begin with, the apparent temperature defined by Eq. (30), is given by

$$T_a = \int_0^{+\infty} dT W(T) T, \quad (35)$$

and is thus equal to the mean temperature of the distribution  $W(T)$ . Hence,  $T_a$  does not depend on the temperature fluctuations variance. The profile is obtained as a weighted sum of Gaussians of different widths, and thus cannot stay rigorously Gaussian itself. Nevertheless, for a sharp temperature PDF peaked around  $T_0$ , the actual deviations from Gaussianity should not be very important, as the dominant contribution in the integral of Eq. (34) is expected to come from the neighborhood of  $T_0$ . However, while leading to accurate results for the central part of the profile, this line of argument is not correct for the line wings. Indeed, the value of  $f(T_0, v_z)$  scales with  $v_z$  as

$$f(T_0, v_z) \propto \exp\left(-\frac{v_z^2}{\xi T_0}\right), \quad (36)$$

and therefore strongly decreases as  $v_z$  increases. Consequently, as shown on Fig. 5, the contribution of the maximum of the temperature PDF in the integral becomes negligible for large enough  $v_z$  (i.e. in the wings of the apparent VDF), and this especially if  $W(T)$  has a slowly decreasing tail.

For instance, an algebraic behavior for the temperature PDF implies a similar one for the measured profile. The relation between the exponents can be obtained in the following manner, noting that for large velocities the apparent VDF can be approximated by

$$f_a(v_z) \sim \int_{v_z^2/\xi}^{+\infty} W(T) \frac{1}{\sqrt{T}} dT. \quad (37)$$

Using then a power-law ansatz for the temperature PDF, the following result is readily obtained

$$W(T) \propto \frac{1}{T^{\alpha+1}} \iff f_a(v_z) \propto \frac{1}{|v_z|^{2\alpha+1}}. \quad (38)$$

For example, let us consider the case in which the temperature fluctuations PDF is the Sinai distribution given by Eq. (27), and plotted in a logarithmic scale on Fig. 2 for  $k = 10$ ,  $T_0 = 30$  eV, and for different values of  $\sigma$  ranging from 5 to 20 eV. The bulk of the apparent VDF remains very close to that of the Maxwellian at 30 eV

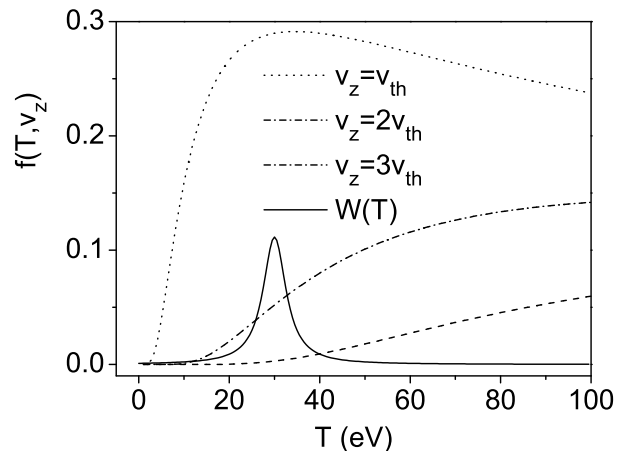


FIG. 5: Plot of the local VDF  $f(T, v_z)$  as a function of  $T$  for three different values of the component of the velocity along the LOS  $v_z = v_{th}, 2v_{th}, 3v_{th}$ , where  $v_{th}$  is the thermal velocity for 30 eV. A model distribution  $W(T)$ , peaked around  $T_0 = 30$  eV is also plotted (solid line). As  $v_z$  is increased, the contribution of  $T_0$  in the calculation of the apparent VDF becomes all the more negligible than the tail of  $W(T)$  decreases slowly.

(dotted line) for every value of  $\sigma$ . However, the discrepancies become important in the apparent VDF tails (i.e. Doppler line wings), all the more so  $\sigma$  is increased. In addition, the tails are found to exhibit a linear behavior in logarithmic scale, which signals a power-law dependence. The exponent which characterizes this algebraic decay should take the value  $-3 - 2/k$  according to Eq. (38). The  $k$  dependence can be checked on Fig. 7 where the apparent VDF is plotted for  $\sigma = 10$  eV and for different values of  $k$  ( $k = 1, 1/2, 10$ ), i.e. different correlation strengths. The stronger the correlations, the larger the deviations from the Maxwellian.

In the frame of the Sinai model, the exponent  $\alpha$  characterizing the apparent VDF power law decay is larger than 3. Other turbulence models could lead to smaller exponents. Let us indeed investigate the case in which the temperature PDF is a Lévy distribution of indexes  $0 < \alpha < 2$  and  $-1 < \beta < 1$ , denoted by  $\mathcal{L}_{\alpha, \beta}(T)$  [32]. In the Fourier space, one has

$$\ln \tilde{\mathcal{L}}_{\alpha, \beta}(k) = -c|k|^\alpha \left( 1 + i\beta \frac{k}{|k|} \omega(k, \alpha) \right), \quad (39)$$

where  $c$  controls the width of the distribution, and the function  $\omega(k, \alpha)$  is defined by

$$\omega(k, \alpha) = \begin{cases} \tan(\pi\alpha/2) & \text{for } \alpha \neq 1, \\ (2/\pi) \ln |k| & \text{for } \alpha = 1. \end{cases}$$

For  $0 < \alpha < 1$  and  $\beta = -1$ ,  $W(T) \equiv 0$  for negative arguments, as should be the case for the temperature

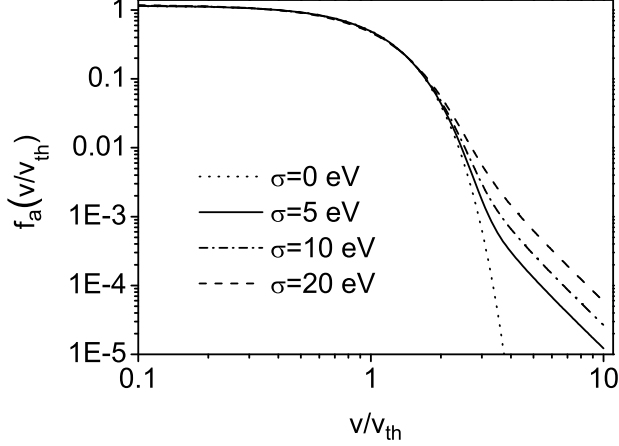


FIG. 6: Plot of the apparent VDF on a logarithmic scale for  $T_0 = 30$  eV,  $k = 10$  and for different values of  $\sigma = 5, 10, 20$  eV.  $v_{th}$  stands for the thermal velocity for  $T = 30$  eV. These plot show the asymptotic power law behavior. The value of the exponent is  $-3.2$  here. The dotted line corresponds to the Gaussian Doppler profile obtained for 30 eV. The deviations from this gaussian profile becomes more and more important as  $\sigma$  grows.

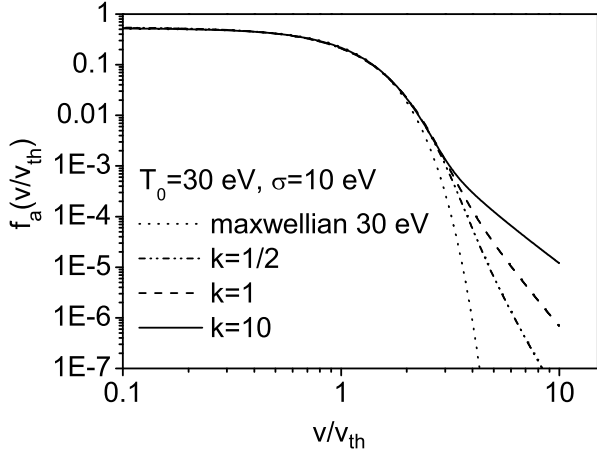


FIG. 7: Plot of the apparent VDF on a logarithmic scale for  $T_0 = 30$  eV,  $\sigma = 10$  eV and for different values of  $k$ ,  $k = 1, 1/2, 10$ .  $v_{th}$  again stands for the thermal velocity for  $T = 30$  eV, and the dotted line corresponds to the Gaussian Doppler profile obtained for 30 eV.

field. The Fourier transform  $\tilde{f}_a(k)$  of the apparent VDF is given by

$$\tilde{f}_a(k) = \int_0^{+\infty} \mathcal{L}_{\alpha,-1}(T) \exp\left(-\frac{\xi T}{4} k^2\right) dT, \quad (40)$$

and can be calculated explicitly using the following result

[32] which gives the Laplace transform of a Lévy distribution

$$\int_0^{+\infty} \mathcal{L}_{\alpha,-1}(T) \exp(-sT) dT = \exp -cs^\alpha, \quad (41)$$

with  $s = k^2/2m + \nu_0$ ,  $m$  standing for the emitters mass. The apparent VDF is thus found to be a symmetrical Lévy distribution of indexes  $\alpha' = 2\alpha$  and  $\beta' = 0$

$$f_a(v) = \frac{\sqrt{2m}}{c^{1/2\alpha}} \mathcal{L}_{2\alpha,0} \left( \frac{\sqrt{2m}}{c^{1/2\alpha}} v \right). \quad (42)$$

Asymptotically,

$$f_a(v) \sim \frac{1}{|v|^{2\alpha+1}}, \quad (43)$$

in accordance with Eq. (38). Here, the value of  $\alpha$  is such that  $1 < 2\alpha + 1 < 3$  and therefore spans a different range than in the Sinai model.

In this idealized model where only temperature fluctuates, the analysis of the apparent VDF tails, i.e. of the line wings, allows to retrieve information on the statistical properties of temperature fluctuations. Indeed, power law decaying tails would for instance be a signature of a similar behavior for the temperature PDF. In addition, in this case, an analysis of the experimental value of the exponent would allow to distinguish between different turbulence models, corresponding for example either to a Sinai or a Lévy PDF.

#### D. Discussion

The study of the case where only one variable fluctuates leads to several enlightening conclusions. First of all, the Doppler profile is only affected by ion temperature and fluid velocity fluctuations along the line of sight, in contrast to the line brightness which essentially reflects the variations of the density. In addition, the bulk of the line appears to be weakly sensitive to the presence of low frequency turbulence, unless the velocity fluctuations variance becomes comparable to the thermal velocity. Therefore, turbulence can indeed be neglected if we restrict ourselves to the study of the core of the line, as is usually done [8, 10, 11]. Conversely, the Doppler line wings behavior is significantly altered by turbulent fluctuations having non-Gaussian PDF. More precisely, long tails for the PDF translates into long tails for the apparent VDF, i.e. slowly decreasing line wings. In this sense, modifications on line wings are associated to intermittency. A comparison with experimental spectra would require further work both from the theoretical and experimental sides, and will not be attempted here. In

particular, a refined model should simultaneously retain velocity and temperature fluctuations. Indeed, velocity and temperature effects cannot be distinguished *a priori*. In fact, examples where fluctuations of both fields lead to a power law behavior for line wings have been presented above. In addition, the couplings between density, velocity and temperature fluctuations, which are responsible for anomalous transport, should also be taken into account. To include these effects in our model, one could either rely on the determination of a joint PDF, or resort to a numerical integration of the fluid equations, which would allow a straightforward calculation of the apparent VDF from Eq. (14). From the experimental point of view, line wings may seem difficult to measure, but it should be kept in mind that the acquisition time can in principle be chosen as large as needed. The only limitation here is the actual duration of the discharge stationary phase during which the measurements are performed.

## VII. APPARENT NON-BOLTZMANN STATISTICS

In the above section, we have shown that the apparent VDF may significantly differ from the Maxwellian calculated using the averaged fields. For the sake of simplicity, let us only consider temperature fluctuations here. The fact that the apparent VDF can be a Lévy distribution highlights a connection between spectroscopy, turbulence and anomalous statistics involving power-law tails, such as the Lévy statistics. Indeed, it should be emphasized that in the case where no other observable than the spectral line shape is available (e.g. in Astrophysics), it is by no mean possible to determine whether the observed plasma is actually turbulent or homogenous. Therefore, if the temperature PDF is a Lévy distribution  $\mathcal{L}_{\alpha,-1}(T)$ , the Doppler spectra might be interpreted as resulting from an homogeneous and stationary plasma governed by Levy statistics. In other words, everything happens as if the plasma under study were in a non-equilibrium stationary state characterized by the Lévy distribution of Eq. (42). This stationary state can be seen as resulting from a relaxation process governed by the following Fractional Fokker-Planck Equation (FFPE) [14, 33, 34]

$$\frac{\partial f_a(v, t)}{\partial t} = \bar{\nu} \frac{\partial}{\partial v} [v f_a] + \bar{D} \frac{\partial^{2\alpha} f_a}{\partial |v|^{2\alpha}}. \quad (44)$$

where  $\bar{\nu}$  and  $\bar{D}$  are such that  $\bar{D}/\bar{\nu} = 2\alpha c/(2m)^\alpha$ . Here, the fractional derivative is defined in the sense of Riesz [32]

$$\frac{\partial^{2\alpha} f_a}{\partial |v|^{2\alpha}} = TF^{-1} \left[ -|k|^{2\alpha} \tilde{f}_{eff} \right]. \quad (45)$$

The usual Fokker-Planck equation (FPE) is recovered for  $\alpha = 1$ . In our case  $\alpha < 1$ , and the apparent VDF cannot

be Gaussian. The main physical difference between the FPE and the FFPE given by Eq. (44) is the spatial non locality of the latter, obvious from the definition of the fractional derivative. This non locality is a consequence of the existence of flights connecting distant regions in the velocity space (the so-called Lévy flights). This property can be traced back to the underlying description of the turbulent plasma. Indeed, at the microscopical scale the trajectory of the radiators can be modelled by a Langevin equation with gaussian white noise [35, 36]. This model describes the collisional relaxation of the local velocity distribution toward the local Maxwellian Eq. (7). Using the fluctuation-dissipation theorem and the expression of the diffusion coefficient stemming from a random walk model [36] leads to

$$\frac{\langle \Delta v^2 \rangle}{\tau_j} \sim \nu \frac{k_B T}{m}, \quad (46)$$

where  $T$  is the local temperature and  $\tau_j$  the typical time between two jumps in the velocity space. Temperature thus determines the characteristic size of jumps in the velocity space. Therefore, high probabilities for large temperature fluctuations in the actual turbulent plasma imply high probabilities for flights in the apparent velocity space. This provides a simple physical picture explaining why the temperature PDF and the apparent VDF asymptotical behavior are linked, and leads to a deeper understanding of Eq. (38). Our results are reminiscent of those presented in references [35, 37, 38], where a similar interpretation of Tsallis non extensive statistical mechanics occurrence was proposed. The latter case arises if the temperature PDF is such that  $1/T$  is gamma distributed [37]. Let us emphasize that in our model, the temperature PDF shape is not arbitrary. In fact, it has to be determined from the fluid equation satisfied by the temperature field in the plasma under consideration, in which relevant expressions for both the source term and the flux have to be specified (see Eq. 6). For each of these expressions, the non-linear character of the latter equation should give rise to a different non-gaussian statistical behavior, i.e. lead to a specific PDF, and therefore to a particular apparent statistics. A natural extension of this work would be to determine what properties fluid equations should have so as to lead to a Lévy distribution for temperature.

## VIII. CONCLUSION AND PERSPECTIVES

In this paper, we have presented a model retaining low frequency turbulence in Doppler line shape calculations. This approach is in particular relevant to the modelling of lines routinely measured in edge plasmas of fusion devices. We have shown that in presence of low frequency turbulence, a straightforward analysis of Doppler profiles yields an apparent velocity distribution function. This apparent VDF is a spatial and time average of the local

VDF. To investigate its shape, we have used a statistical description of the plasma turbulent fluctuations, relevant whenever the acquisition time of the spectrometer is large with respect to the typical turbulent time scale. The resulting expression for the apparent VDF involves the joint Probability Density Function of the fluctuating fields. Next, considering the case where only one variable fluctuates, we have obtained several new results. While density fluctuations do not affect Doppler line shapes, velocity or ion temperature fluctuations can strongly influence line wings. This is especially the case when their PDF have long tails such as power laws. It might therefore be possible to diagnose such a behavior by the mean of line shapes, once Stark effect has been carefully ruled out. A reliable comparison with experiments would imply dedicated measurements which are not yet available, but also further modelling. In particular, the use of a turbulence code would be very helpful for diagnosis purposes, and this possibility will be investigated in a future work. From a more fundamental point of view, our work

sheds light on some possible connections between turbulence, spectroscopy and non Boltzmann statistics, such as those involving Lévy or Tsallis distributions. Our approach furthermore relates the occurrence of one of these particular statistics to the properties of the fluid equations describing turbulence. Our model thus provides a frame to investigate both experimentally and theoretically some of the fundamentals aspects of the statistical properties of the physical observables in out of equilibrium plasmas.

### Acknowledgments

The authors would like to thank F. B. Rosmej for helpful discussions. This work is part of a collaboration (LRC DSM 99-14) between the Laboratoire de Physique des Interactions Ioniques et Moléculaires and the Département de Recherches sur la Fusion Contrôlée, CEA Cadarache.

- 
- [1] J. A. Krommes, *Physics Reports* **360**, 1 (2002).
- [2] X. Garbet, *Plasma Phys. Control. Fusion* **43**, A251 (2001).
- [3] W. Horton, *Rev. Mod. Phys.* **71**, 735 (1999).
- [4] H. R. Griem, *Spectral Line Broadening by Plasmas* (Academic Press New York and London, 1974).
- [5] E. Oks, *Plasma Spectroscopy* (Springer-Verlag, Berlin Heidelberg, 1995).
- [6] H. Capes and D. Voslamber, *Phys. Rev. A* **15**, 1751 (1977).
- [7] M. Baranger and B. Mozer, *Phys. Rev.* **123**, 25 (1961).
- [8] H. Kubo, H. Takenaga, T. Sugie, S. Higashijima, S. Suzuki, A. Sakasai, and N. Hosogane, *Plasma Phys. Control. Fusion* **40**, 1115 (1998).
- [9] D. P. Stotler, C. H. Skinner, R. V. Budny, A. T. Ramsey, D. N. Ruzic, and J. R. B. Turkot, *Phys. Plasmas* **3**, 4084 (1996).
- [10] J. D. Hey, C. C. Chu, and E. Hintz, *J. Phys. B: At. Mol. Opt. Phys.* **32**, 3555 (1999).
- [11] M. Koubiti, Y. Marandet, A. Escarguel, H. Capes, L. Godbert-Mouret, R. Stamm, C. D. Michelis, R. Guirlet, and M. Mattioli, *Plasma Phys. Control. Fusion* **44**, 261 (2002).
- [12] Y. Marandet, P. Genesio, M. Koubiti, L. Godbert-Mouret, B. Felts, R. Stamm, H. Capes, and R. Guirlet, *Nuc. Fus.* **44**, S118 (2004).
- [13] Y. Marandet, H. Capes, L. Godbert-Mouret, M. Koubiti, and R. Stamm, *Europhys. Lett.* (2005), accepted for publication.
- [14] Y. Marandet, H. Capes, L. Godbert-Mouret, R. Guirlet, M. Koubiti, and R. Stamm, *Communications in non linear science and numerical simulations* **8**, 469 (2003).
- [15] G. M. Zaslavsky, M. Edelman, H. Weitzner, B. Carreras, G. McKee, R. Bravenec, and R. Fonck, *Phys. Plasmas* **7**, 3691 (2000).
- [16] M. Jakubowski, R. J. Fonck, and G. R. Mckee, *Phys. Rev. Lett.* **89**, 265003 (2002).
- [17] F. B. Rosmej, H. Capes, M. Koubiti, V. Lisitsa, Y. Marandet, A. Meigs, and R. Stamm, *Europhysics Conference Abstract* **27A**, 1.176 (2003).
- [18] S. G. Rautian and I. I. Sobel'man, *Soviet Physics Uspekhi* **9**, 701 (1967).
- [19] B. H. Bransden and C. J. Joachain, *Physic of atoms and molecules* (Longman Scientific and Technical, 1983).
- [20] U. Frisch, *Turbulence* (Cambridge University Press, 1995).
- [21] S. B. Pope, *Turbulent Flows* (Cambridge University Press, 2000).
- [22] H. Chen, S. Chen, and R. H. Kraichnan, *Phys. Rev. Lett.* **63**, 2657 (1989).
- [23] A. Das and P. Kaw, *Phys. Plasmas* **2**, 1497 (1995).
- [24] Y. G. Sinai and V. Yakhot, *Phys. Rev. Lett* **63**, 1962 (1989).
- [25] C. Tsallis, *Chaos* **6**, 539 (1995).
- [26] H. R. Griem, *Principles of Plasma Spectroscopy*, Cambridge Monographs on Plasma Physics (Cambridge University Press, 1997).
- [27] A. Unsöld, *Physik des Sternatmosphären* (Springer-Verlag, Berlin, 1955).
- [28] N. A. Iganov and R. A. Sunyaev, *Astronomy Letters* **29**, 791 (2003).
- [29] M. D. Ding et al., *Astron. Astrophys.* **348**, L29 (1999).
- [30] Y. Liu and M.-D. Ding, *Chin. J. Astron. Astrophys.* **2**, 277 (2002).
- [31] R. Jha et al., *Phys. Plasmas* **10**, 699 (2003).
- [32] W. Paul and J. Baschnagel, *Stochastic processes, From Physics to finance* (Springer-Verlag, 1999).
- [33] S. Jespersen, R. Metzler, and H. C. Fogedby, *Phys. Rev. E* **59**, 2736 (1999).
- [34] A. V. Chechkin and V. Y. Gonchar, *Phys. Plasmas* **9**, 78 (2002).
- [35] C. Beck, *Phys. Rev. Lett.* **187601** (2001).
- [36] P. Resibois and M. DeLeener, *Classical Kinetic Theory of fluids* (Wiley-Interscience, 1977).
- [37] G. Wilk and Z. Wlodarczyk, *Phys. Rev. Lett.* **84**, 2770 (2000).

[38] C. Beck and E. D. G. Cohen, *Physica A* **322**, 267 (2003).